

# LONGITUDINAL BEAM DYNAMICS INVESTIGATIONS AT THE GSI UNILAC FOR NON-RELATIVISTIC ION BEAMS

N. Schmidt<sup>\*1, 2, 3</sup>, M. Miski-Oglu<sup>1, 3, 4</sup>, P. Forck<sup>1</sup>, S. Klaproth<sup>5</sup>, S. Lauber<sup>6</sup>,  
U. Scheeler<sup>1</sup>, R. Singh<sup>1</sup>, S. Yaramyshev<sup>1</sup>, W. Barth<sup>1, 4</sup>

<sup>1</sup>GSI Helmholtz Center for Heavy Ion Research, Darmstadt, Germany

<sup>2</sup>Technical University of Darmstadt, Germany

<sup>3</sup>Helmholtz Institute Mainz, Germany

<sup>4</sup>Johannes Gutenberg University Mainz, Germany

<sup>5</sup>Technische Hochschule Mittelhessen, Friedberg, Germany

<sup>6</sup>CERN, Geneva, Switzerland

## Abstract

At the heavy-ion accelerator UNiversal Linear ACcelerator (UNILAC) at GSI Helmholtz Center for Heavy Ion Research (GSI) in Darmstadt, measurements of the longitudinal emittance were performed using a Fast Faraday Cup (FFC) installed in a dispersive section. The FFC provides high-resolution, time-resolved measurements of the charge distribution along the longitudinal beam profile. Different buncher settings were applied to study the longitudinal beam dynamics and identify the phase and energy foci at the FFC location. Based on these measurements, beam dynamics calculations were carried out to determine the longitudinal emittance at the exit of the Alvarez section. Measurement and calculation results will be presented.

## INTRODUCTION

In addition to transverse extent and divergence, the longitudinal charge distribution within an ion bunch is one of the most important properties of a beam in linear accelerators. This is determined by the bunch shape and length, as well as the beam's energy spread. These factors influence the beam transmission and, consequently, the efficiency of the accelerator. Generally, experiments require a low uncertainty of the ion beam energy; therefore, it is important to measure the charge distribution in the longitudinal phase plane.

Typically, one determines the 2D bunch portrait in the longitudinal phase plane by measuring one of the projections under controlled longitudinal optics settings [1]. Given that, the UNiversal Linear ACcelerator (UNILAC) [2–7], see Fig. 1, at GSI Helmholtz Centre for Heavy-Ion Research

is equipped with various instruments for longitudinal beam diagnostics, including the Fast Faraday Cup (FFC). FFCs are variants of the regular Faraday Cups optimized for measuring fast time-varying charge distributions in the nanosecond regime.

The objective of this work is the determination of the longitudinal emittance behind the Alvarez section using the Dispersion-Assisted Longitudinal Emittance (DALE) measurement method [8]. When charged particle beams pass through a dispersive section, particles with different kinetic energies are deflected on different trajectories. Hence, in circumstances where the dispersion is sufficiently large, the energy spread can be translated into transverse deflection, which then can be scanned with the movable FFC. Since the section of the Alvarez cavities themselves is not dispersive, the data presented here was recorded in the dispersive beamline at the X2 target location in the experimental hall at the UNILAC exit using a Radially Coupled Fast Faraday Cup (RCFFC) in July 2025. The particle ensembles, generated from the measurements, were subsequently back-propagated to the exit of the Alvarez section using the multi-particle tracking code Aperture3D [9].

This paper provides a brief introduction to the functionality of the RCFFC, the experimental setup, and the methods employed. The focus lies on the ion beam measurements of the charge distribution in the longitudinal phase plane. Furthermore, the backpropagation of the obtained ion distribution is presented.

## FAST FARADAY CUP

The RCFFC is capable of measuring the longitudinal charge distribution of each bunch along the macro pulse.

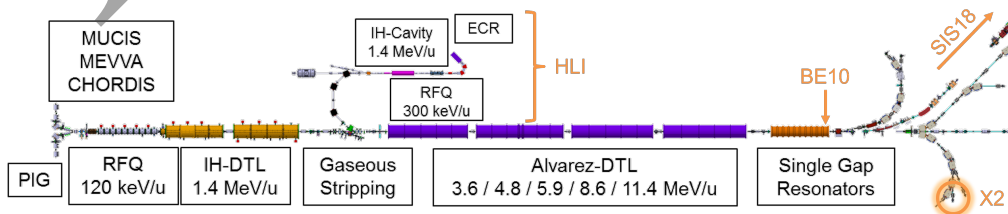


Figure 1: Layout of the UNILAC. The target location X2 and the buncher BE10 adjusted for this measurement are highlighted [7].

\* nim.schmidt@gsi.de

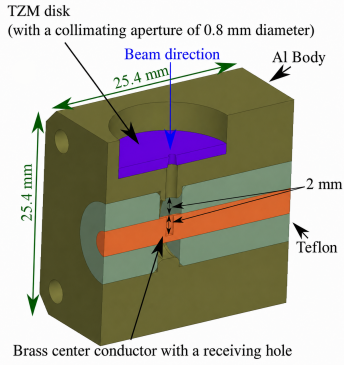


Figure 2: Cross-section view of the RCFFC. The beam incidence is indicated [10].

The beam couples through a round hole from the side of a coaxial cable through the dielectric medium into the central conductor. It has a bandwidth of 5 GHz and a time resolution of 22 ps at  $\beta = 0.15$  limited by field dilution effects [11–14]. In order to minimize the leakage of Secondary Electrons (SEs), the hole is designed with a width of 1 mm and depth of 2.5 mm, see Fig. 2. Additionally, positive biasing is applied on the collector of the RCFFC to further suppress SEs. The hole in the outer conductor of the co-axial is covered with a Titanium-Zirconium-Molybdenum alloy (TZM) disk with a 0.8 mm hole with the purpose of tolerating the heat deposited by the beam and reducing field dilution effects [10].

## MEASUREMENTS

The measurements presented in this work were carried out with a  $Ar^{8+}$  ion beam from the high charge state injector (HLI) with an energy of 11.4 MeV/u and an average beam current of 35  $\mu A$  at the X2 target location (see Fig. 1). The RCFFC is measuring the longitudinal charge distribution bunch-by-bunch in the macro pulse. Fig. 3 shows the average distribution of all bunches in one pulse.

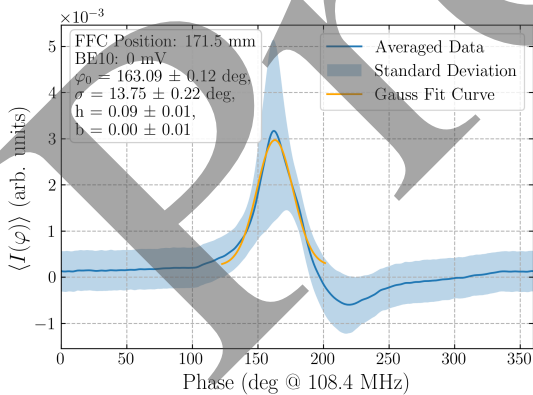


Figure 3: The average longitudinal charge distribution of a 35  $\mu A$   $Ar^{8+}$  at the X2 target location at the UNILAC.

The negative spike in intensity at the bunch tail originates mainly from the AC coupling of the broadband amplifiers (50 MHz - 6 GHz) with additional contributions from SE emission. The band arises due to intensity fluctuations within the pulse. The bunch phase width was measured to

be  $\sigma = 13.75$  deg, which corresponds to a time structure of  $\sigma = 352$  ps at a frequency of  $f = 108.4$  MHz. However, it should be noted that this only corresponds to the bunch length of a transversal slice of the beam, as only a part of the beam passes through the hole of 0.8 mm in the RCFFC. The measurement of the entire beam, horizontally scanned with the stepper motor driven FFC, is shown in Fig. 4.

The inverse of the dispersion at the X2 target location was determined to be 9.16 keV/(u mm) using the multi-particle tracking code Aperture3D with the accelerator settings employed. In addition, the dispersion was experimentally determined by measuring the horizontal beam profile and change of its center as a function of beam energy. The values determined using the two methods are consistent with one another. This value can be used to associate the FFC stepper motor positions with specific particle energies, with higher position values corresponding to higher-energy particles, as shown in Fig. 4. The measured charge distributions in the longitudinal phase plane reveal two central energy peaks that probably originate in the HLI.

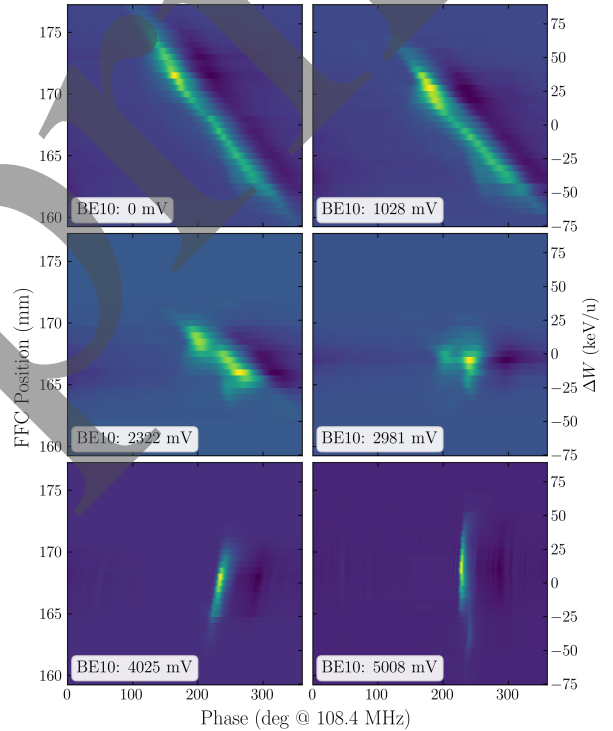


Figure 4: Measurements of the charge distribution in the longitudinal phase plane for different buncher amplitudes in bunching mode.

In order to verify that the charge distribution in the longitudinal phase plane had indeed been measured and to test the possibility of beam manipulation, the single gap resonator BE10 was used as a buncher. The buncher amplitude was then gradually increased. For each of these dedicated settings, the entire beam was scanned horizontally with the FFC in order to measure the charge distribution in the longitudinal phase plane. A set of such distributions obtained through this method is presented in Fig. 4. It is evident from the data set that there is a clear and perceptible transformation of the

particle ensemble with increasing buncher amplitudes. In bunching mode, particles that arrive first are decelerated by the RF-field, whilst those with later arrival times are accelerated. The buncher amplitude directly correlates with the strength of this force acting on the beam. The beam line between the buncher and the FFC in X2 contains several dipole and quadrupole magnets. To illustrate a transformation of the ellipse, representing the beam portrait in the longitudinal phase plane, a drift of 29 m is used, where higher-energy particles arrive earlier while lower-energy particles arrive later as shown in Fig. 5.

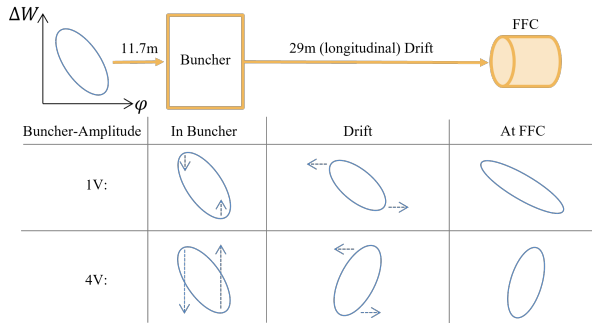


Figure 5: Transformation of the ellipse, representing the beam portrait in the longitudinal phase plane for different buncher settings. The arrows indicate the direction of the transformation in the buncher and the 29 m long drift.

The targeted beam manipulation is clearly recognizable in Fig. 4, demonstrating the sensitivity of the longitudinal beam dynamics to the applied buncher settings and thereby verifying the feasibility of this approach.

## BACKPROPAGATION

Building on this, the particle distributions constructed from the data sets were back-propagated from the measurement point in the diagnostic chamber in X2 to the exit of the Alvarez section for the respective buncher settings using the multiparticle beam dynamics code *Aperture3D*. Additionally, the 4-RMS ellipses of the back-propagated particle ensembles were then calculated; see Fig. 6. The orientations of the corresponding ellipses show good agreement within  $\pm 2.5\%$ . However, they differ in phase width and emittance, which might be explained by higher particle losses at higher buncher amplitudes.

In addition, an average ellipse was characterized by averaging the Twiss parameters of all ellipses. This is shown in black in Fig. 6. Furthermore, another ellipse was determined that encloses all ellipses under consideration, shown in grey in Fig. 6. Although a complete agreement between all the ellipses is not achieved, it must be assumed that the particle ensemble actually expected in the longitudinal phase plane behind the Alvarez section lies within this “overall ellipse” with a longitudinal 4-RMS emittance of  $4 \cdot \epsilon_{\text{rms}} = 2800 \text{ deg keV/u}$ .

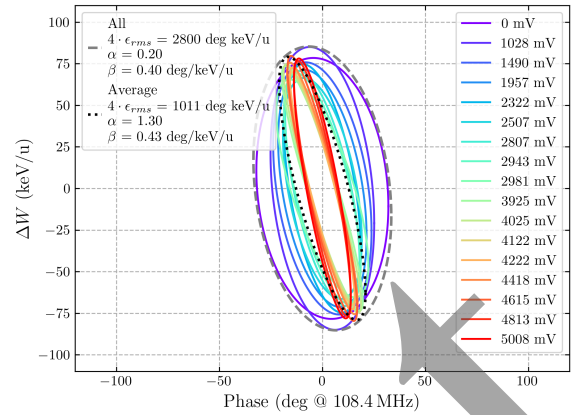


Figure 6: 4-RMS ellipses of the back-propagated particle ensembles of various data sets at the exit of the Alvarez section, marked by the buncher voltage applied during the respective measurement.

## CONCLUSION & OUTLOOK

The charge distribution in the longitudinal phase plane at the UNILAC exit was successfully characterized using dispersion-assisted longitudinal emittance measurements with the RCFFC. By systematically varying the buncher settings, the beam shape could be manipulated, and the expected transformation was clearly observed, confirming the validity of the method.

Building on this, the particle ensembles, generated from the experimentally determined data, were back-propagated from the measurement point in the diagnostic chamber in X2 to the exit of the Alvarez section. At this position, a maximum longitudinal RMS emittance of  $\epsilon_{\text{rms}} = 700 \text{ deg keV/u}$  could be calculated.

The obtained results allow further optimization of the beam injection into the synchrotron SIS18 [15]. In addition, the developed method could potentially be used in the superconducting, continuous wave, heavy ion accelerator HELIAC [16–19], which is currently under construction at GSI and Helmholtz Institute Mainz.

## ACKNOWLEDGEMENTS

We thank S. Loechner, T. Milosic, H. Vormann and the UNILAC operators for their dedicated support in accelerator operation and experimental preparation, as well as for their valuable assistance throughout the measurements. We acknowledge the discussions on the design of FFC with A. Shemyakin and D. Sun from Fermilab.

## REFERENCES

- [1] S. Lauber *et al.*, “Longitudinal phase space reconstruction for a heavy ion accelerator”, *Phys. Rev. Accel. Beams*, vol. 23, p. 114201. [doi:10.1103/PhysRevAccelBeams.23.114201](https://doi.org/10.1103/PhysRevAccelBeams.23.114201)
- [2] W. Barth *et al.*, “High brilliance beam investigations at the universal linear accelerator”, *Phys. Rev. Accel. Beams*, vol.

- 25, p. 040101.  
[doi:10.1103/PhysRevAccelBeams.25.040101](https://doi.org/10.1103/PhysRevAccelBeams.25.040101)
- [3] W. Barth *et al.*, “High brilliance uranium beams for the GSI FAIR”, *Phys. Rev. Accel. Beams*, vol. 20, p. 050101.  
[doi:10.1103/PhysRevAccelBeams.20.050101](https://doi.org/10.1103/PhysRevAccelBeams.20.050101)
- [4] S. Yaramyshev *et al.*, “DYNAMION—A Powerful Beam Dynamics Software Package for the Development of Ion Linear Accelerators and Decelerators”, *Applied Sciences*, vol. 13, p. 8422. [doi:10.3390/app13148422](https://doi.org/10.3390/app13148422)
- [5] W. Barth *et al.*, “U<sup>28+</sup>-intensity record applying a H<sub>2</sub>-gas stripper cell”, *Phys. Rev. Spec. Top. Accel. Beams*, vol. 18, p. 040101. [doi:10.1103/PhysRevSTAB.18.040101](https://doi.org/10.1103/PhysRevSTAB.18.040101)
- [6] W. Barth *et al.*, “Heavy ion linac as a high current proton beam injector”, *Phys. Rev. Spec. Top. Accel. Beams*, vol. 18, p. 050102. [doi:10.1103/PhysRevSTAB.18.050102](https://doi.org/10.1103/PhysRevSTAB.18.050102)
- [7] GSI UNILAC Overview, <https://www.gsi.de/work/beschleunigerbetrieb/beschleuniger/unilac/unilac>
- [8] R. Singh, “Longitudinal Beam Diagnostics R&D at GSI-UNILAC”, in *Proc. HIAT’22*, Darmstadt, Germany, Jun.-Jul. 2022, pp. 144–149.  
[doi:10.18429/JACoW-HIAT2022-TH2I2](https://doi.org/10.18429/JACoW-HIAT2022-TH2I2)
- [9] S. Lauber *et al.*, “Modeling beam dynamics in the HELIAC Advanced Demonstrator”, in *Proc. LINAC’24*, Chicago, IL, USA, Aug. 2024, pp. 404–407.  
[doi:10.18429/JACoW-LINAC2024-TUPB031](https://doi.org/10.18429/JACoW-LINAC2024-TUPB031)
- [10] J.-P. Carniero *et al.*, “Longitudinal beam dynamics studies at the PIP-II injector test facility”, *Int. J. Mod. Phys. A*, vol. 34, no. 36, p. 1942013, Dec. 2019.  
[doi:10.1142/s0217751x19420132](https://doi.org/10.1142/s0217751x19420132)
- [11] R. Singh *et al.*, “Simulation and Measurements of the Fast Faraday Cups at GSI UNILAC”, in *Proc. IBIC’22*, Kraków, Poland, Sep. 2022, pp. 286-290.  
[doi:10.18429/JACoW-IBIC2022-TUP25](https://doi.org/10.18429/JACoW-IBIC2022-TUP25)
- [12] S. Klapproth *et al.*, “RF Characterization and Beam Measurements with Additively Manufactured Fast Faraday Cups”, *Instruments* 2025, vol. 9, p. 32.  
[doi:10.3390/instruments9040032](https://doi.org/10.3390/instruments9040032)
- [13] A. Shemyakin, “Estimation of dilution of a Fast Faraday Cup response due to the finite particles speed”.  
[doi:10.48550/arXiv.1612.09539](https://doi.org/10.48550/arXiv.1612.09539)
- [14] K. Mal, S. Kumar, G. Rodrigues, and R. Singh, “Study and improvements of a radially coupled coaxial Fast Faraday cup design toward lower intensity beams”, *AIP Adv.*, vol. 12, no. 12, Dec. 2022. [doi:10.1063/5.0131890](https://doi.org/10.1063/5.0131890)
- [15] S. Appel, “SIS18 - Parameter Studies on MTI Efficiency with Space Charge and Longitudinal Aspects”, talk at the *GSI FAIR Injector Review*, 2013
- [16] W. Barth *et al.*, “First heavy ion beam tests with a superconducting multigap CH cavity”, *Phys. Rev. Accel. Beams*, vol. 21, p. 020102.  
[doi:10.1103/PhysRevAccelBeams.21.020102](https://doi.org/10.1103/PhysRevAccelBeams.21.020102)
- [17] M. Schwarz *et al.*, “Reference beam dynamics layout for the SC CW heavy ion HELIAC at GSI”, *Nucl. Instrum. Methods Phys. Res., Sect. A*, vol. 951, p. 163044.  
[doi:10.1016/j.nima.2019.163044](https://doi.org/10.1016/j.nima.2019.163044)
- [18] S. Lauber *et al.*, “An Alternating Phase Focusing injector for heavy ion acceleration”, *Nucl. Instrum. Methods Phys. Res., Sect. A*, vol. 1040, p. 167099.  
[doi:10.1016/j.nima.2022.167099](https://doi.org/10.1016/j.nima.2022.167099)
- [19] M. Basten *et al.*, “High brilliance uranium beams for the GSI FAIR”, *Rev. Sci. Instrum.*, vol. 93, p. 063303.  
[doi:10.1063/5.0094859](https://doi.org/10.1063/5.0094859)